ON THE ASYMPTOTIC RESOLVABILITY OF FAR-FIELD STOCHASTIC SOURCES

Xin Zhang, Mohammed Nabil El Korso and Marius Pesavento

Communication Systems Group, Technische Universität Darmstadt
Darmstadt, Germany

ABSTRACT

The resolvability of two closely spaced signals is an important performance measure for parametric estimation problems. In this paper, we investigate the minimum signal-to-noise ratio, denoted by $\mathrm{SNR}_{\min}$, required to correctly resolve two closely spaced stochastic sources in the far-field context. As a by-product, we first derive an analytical expression of the stochastic Cramér-Rao bound (CRB) with respect to the separation parameter (i.e., we consider a new parametrization where one source is fixed). Then using the Smith criterion, we derive a closed-form expression of the $\mathrm{SNR}_{\min}$. Our analytical expression reveals some insightful properties that are discussed in detail and, finally, numerical examples are provided to corroborate the proposed theoretical analysis.

Index Terms— Stochastic Cramér-Rao bound, statistical resolution limit, minimum signal-to-noise ratio

1. INTRODUCTION

The problem of far-field source localization by an array of sensors is a significant topic with numerous applications including radar, sonar, wireless communications [1], etc. One of the most important measures to quantify the performance for this parameter estimation problem is the resolvability of closely spaced signals in terms of their parameter of interest. In this paper, we aim to investigate the relationship between the resolvability and the signal-to-noise ratio by focusing on the following question: "*What is the minimum signal-to-noise ratio required for a sensor array to correctly resolve two closely spaced far-field stochastic signals for a given distance between them?*"

To address the above question, we firstly revise the concept of the statistical resolution limit (SRL), which is a common tool to characterize the resolvability of two signals. The SRL is generally defined as the minimum distance with respect to the parameter of interest (e.g. the directions-of-arrival (DOA), electrical angles, etc.), that allows distinguishing between two closely spaced sources [2–4]. There exist three fundamental approaches to describe the SRL. The first is based on the analysis of the mean null spectrum (i.e., it is related to a specific high-resolution algorithm) [5], the second on the detection theory [6, 7], and the third on the estimation theory, employing the Cramér-Rao bound (CRB) [2, 8, 9]. One widely used criterion for the SRL based on CRB was proposed by Smith [2], and states that *two signals are revolvable if the distance (w.r.t. the parameter of interest) between them is greater than the standard deviation of the distance estimation*. Therefore, the SRL is associated with a minimum required signal-to-noise ratio, denoted by $\mathrm{SNR}_{\min}$, to correctly resolve two closely spaced sources. In this paper we consider the SRL in the Smith sense for the following reasons. *i*) The Smith criterion is preferable to other criteria related to the third approach, e.g., the one proposed in [8], since it takes into account the coupling between the parameters. *ii*) Furthermore, a known drawback of the mean null spectrum approach is that it is designed for a specific high-resolution algorithm, and, *iii*) on the other hand, the SRL based on the hypothesis test approach is related to that based on the Smith criterion [4]. The main objective of this paper is to derive an explicit, analytical expression of $\mathrm{SNR}_{\min}$ representing this relationship for a large number of snapshots. As a by-product, a closed-form expression of the stochastic CRB (w.r.t. the source separation) is derived, which serves to obtain the analytical expression of $\mathrm{SNR}_{\min}$. The CRB derived in this paper is based on a different parametrization than the commonly used one (where we consider one source to be fixed and the separation between the two sources to be the unknown parameter of interest) and is, to the best of our knowledge, absent in the current literature. Finally one should note that our analytical expression reveals some insightful information related to the behavior of $\mathrm{SNR}_{\min}$. Furthermore, it is computationally efficient for large number of sensors (i.e., by saving the trouble of inverting the data covariance matrix).

This paper is organized as follows. In Section 2, we introduce the observation model and the related assumptions concerning the parametrization. Section 3 is mainly dedicated to the derivation of the stochastic CRB and of the $\mathrm{SNR}_{\min}$. In Section 4, simulation results are presented to validate our analytical derivation. We also provide a discussion on some insightful properties revealed by the result of the simulations. Finally, in Section 5, we summarize our work and provide some concluding comments.

The following notation will be employed throughout this paper: $(\cdot)^H$, $(\cdot)^*$ and $(\cdot)^T$ denote the conjugate transpose, the conjugate and the transpose of a matrix, respectively. $tr\{\cdot\}$ and $vec\{\cdot\}$ denote the trace and the vectorization of a matrix, respectively. $\Re\{\cdot\}$ and $\Im\{\cdot\}$ denote the real and imaginary part respectively. $\otimes$ denotes the Kronecker product, whereas $E\{\cdot\}$ denotes the expectation.

2. PROBLEM FORMULATION

Consider a linear array, not necessarily uniform, comprising M sensors, on which two far-field narrowband stochastic signals $s_1(t)$ and $s_2(t)$ impinge with directions-of-arrival θ_1 and $\theta_1+\delta$, respectively, where δ denotes the spacing between the DOAs of the two sources. The received signal at the m-th sensor, denoted by $x_m(t)$, can be expressed as [1]:

$$\begin{aligned} x_m(t) =& s_1(t)e^{jkd_m\sin(\theta_1)} + s_2(t)e^{jkd_m\sin(\theta_1+\delta)} \\ &+ n_m(t), t=1,...,N \text{ and } m=1,...,M. \end{aligned} \tag{1}$$

where d_m is the spacing between the first sensor (which is chosen as the so-called reference sensor, i.e., $d_1=0$) and the m-th sensor, $k=\frac{2\pi}{\lambda}$ is the wave number (with λ denoting the wave length), $n_m(t)$ denotes the additive noise at the m-th sensor, and N is the number of snapshots.

The vector representation of (1) is given by:

$$\boldsymbol{x}(t) = \boldsymbol{A}\boldsymbol{s}(t) + \boldsymbol{n}(t), \tag{2}$$

where $\boldsymbol{x}(t) = [x_1(t),...,x_M(t)]^T$, $\boldsymbol{s}(t) = [s_1(t), s_2(t)]^T$, $\boldsymbol{n}(t) = [n_1(t),...,n_M(t)]^T$, and $\boldsymbol{A} = [\boldsymbol{a}(\theta_1), \boldsymbol{a}(\theta_1+\delta)]$. The vectors $\boldsymbol{a}(\theta_1)$ and $\boldsymbol{a}(\theta_1+\delta)$ represent the steering vectors of the array w.r.t. directions θ_1 and $\theta_1+\delta$, respectively, which are defined as $\boldsymbol{a}(\theta_1) = [1, e^{jkd_2\sin(\theta_1)},...,e^{jkd_M\sin(\theta_1)}]^T$ and $\boldsymbol{a}(\theta_1+\delta) = [1, e^{jkd_2\sin(\theta_1+\delta)},...,e^{jkd_M\sin(\theta_1+\delta)}]^T$.

The following assumptions are made in the remaining of the paper:

A1 The sensor noise follows a complex circular white Gaussian distributed, both spatially and temporally, with zero-mean and unknown noise variance σ^2.

A2 The source signals are temporally white zero-mean Gaussian processes whose covariance matrix is denoted by $\boldsymbol{S} = \begin{bmatrix} \sigma_1^2 & \rho \\ \rho^* & \sigma_2^2 \end{bmatrix}$, where σ_1^2 and σ_2^2 denote the variances of the two source signals, respectively, $\rho_c = \frac{\rho}{\sigma_1\sigma_2}$ is the correlation coefficient between the two signals. Further we assume that the source signals and noise signals are mutually independent.

A3 The unknown parameter vector is[1] $\boldsymbol{\xi} = \left[\delta, \boldsymbol{\varsigma}^T, \sigma^2\right]^T$, where $\boldsymbol{\varsigma} = [\sigma_1, \sigma_2, \Re\{\rho\}, \Im\{\rho\}]^T$; and the number of snapshots is assumed to be large.

[1]In this paper θ_1 can be viewed as a known parameter. The case of unknown θ_1 is beyond the scope of this paper.

3. DERIVATION OF SNR$_{\min}$

The derivation of the SNR$_{\rm min}$ can be divided roughly into two steps. The first step is the derivation of the stochastic CRB w.r.t. δ; the second is the utilization of the Smith criterion, leading to the final expression of the SNR$_{\rm min}$.

To the best of our knowledge there is no closed-form expression at hand suiting our purpose and, hence, entails a new derivation of the stochastic CRB w.r.t. the model described by (1). The obtained expression serves as the cornerstone to obtain the closed-expression of the SNR$_{\rm min}$.

The derivation of CRB(δ) follows principally the same train of thought as that in [10], and gives the following result:

$$\text{CRB}(\delta) = \frac{\sigma^2}{2N} \cdot \frac{1}{\boldsymbol{d}_\delta^H \boldsymbol{\Pi}_{\boldsymbol{A}}^\perp \boldsymbol{d}_\delta \boldsymbol{c}_\rho^H \boldsymbol{A}^H \boldsymbol{R}^{-1} \boldsymbol{A} \boldsymbol{c}_\rho}. \tag{3}$$

with $\boldsymbol{c}_\rho = \left[\rho, \sigma_2^2\right]^T$ and $\boldsymbol{d}_\delta = \frac{\partial \boldsymbol{a}(\theta_1+\delta)}{\partial\delta}$. For the details of the derivation please refer to the appendix of this paper.

Now consider the SRL defined by the Smith's criterion: *Two signals are revolvable if the distance (w.r.t the parameter of interest) between them is greater than the standard deviation of the distance estimation*, i.e., δ is given as the solution of the following equation:

$$\delta^2 = \text{CRB}(\delta). \tag{4}$$

From (4) we shall derive the expression of the SNR$_{\rm min}$ for a large number of snapshots, since it is evident that the SNR for which (4) holds corresponds to SNR$_{\rm min}$. To make our aim accessible, we have to simplify the expression of CRB(δ) using appropriate mathematical manipulations and approximations. Based on **A1** and **A2** the data covariance matrix $\boldsymbol{R} = \mathrm{E}\{\boldsymbol{x}(\mathrm{t})\boldsymbol{x}^{\mathrm{H}}(\mathrm{t})\}$ can be expressed as:

$$\boldsymbol{R} = \boldsymbol{A}\boldsymbol{S}\boldsymbol{A}^H + \sigma^2\boldsymbol{I}. \tag{5}$$

where $\boldsymbol{I}$ is defined as the identity matrix. Resorting to the Woodbury matrix identity [11] we obtain

$$\begin{aligned} \boldsymbol{R}^{-1} &= (\boldsymbol{A}\boldsymbol{S}\boldsymbol{A}^H + \sigma^2\boldsymbol{I})^{-1} \\ &= \frac{1}{\sigma^2}\left(\boldsymbol{I} - \frac{1}{\sigma^2}\boldsymbol{A}(\boldsymbol{S}^{-1} + \boldsymbol{A}^H\frac{1}{\sigma^2}\boldsymbol{A})^{-1}\boldsymbol{A}^H\right) \\ &= \frac{1}{\sigma^2}\left(\boldsymbol{I} - \boldsymbol{A}(\sigma^2\boldsymbol{S}^{-1} + \boldsymbol{A}^H\boldsymbol{A})^{-1}\boldsymbol{A}^H\right). \end{aligned} \tag{6}$$

For a sufficient SNR (i.e., for a small σ^2), $\boldsymbol{R}^{-1}$ can be approximated[2] as [11, eq. (177)]:

$$\begin{aligned} \boldsymbol{R}^{-1} &= \frac{1}{\sigma^2}\left(\boldsymbol{I} - \boldsymbol{A}(\sigma^2\boldsymbol{S}^{-1} + \boldsymbol{A}^H\boldsymbol{A})^{-1}\boldsymbol{A}^H\right) \\ &\approx \frac{1}{\sigma^2}\left(\boldsymbol{I} - \boldsymbol{A}\left((\boldsymbol{A}^H\boldsymbol{A})^{-1} - \sigma^2(\boldsymbol{A}^H\boldsymbol{A})^{-1}\boldsymbol{S}^{-1}(\boldsymbol{A}^H\boldsymbol{A})^{-1}\right)\boldsymbol{A}^H\right) \\ &= \frac{1}{\sigma^2}\left(\boldsymbol{I} - \boldsymbol{A}\boldsymbol{A}^\sharp\right) + (\boldsymbol{A}^\sharp)^H\boldsymbol{S}^{-1}\boldsymbol{A}^\sharp \\ &= \frac{1}{\sigma^2}\boldsymbol{\Pi}_{\boldsymbol{A}}^\perp + (\boldsymbol{A}^\sharp)^H\boldsymbol{S}^{-1}\boldsymbol{A}^\sharp, \end{aligned} \tag{7}$$

[2]Note that in our application this approximation is tight, since our numerical simulation demonstrates that the SNR$_{\rm min}$ obtained based on this approximation is in a good agreement with that acquired numerically, as is illustrated later in Fig. 1.

where $\boldsymbol{A}^{\sharp} = (\boldsymbol{A}^H\boldsymbol{A})^{-1}\boldsymbol{A}^H$ denotes the Moore-Penrose pseudoinverse of $\boldsymbol{A}$. Consequently in the denominator of the expression (3) we have,

$$\begin{aligned} &\boldsymbol{c}_\rho^H\boldsymbol{A}^H\boldsymbol{R}^{-1}\boldsymbol{A}\boldsymbol{c}_\rho = \boldsymbol{c}_\rho^H\boldsymbol{S}^{-1}\boldsymbol{c}_\rho \\ =&\frac{1}{\sigma_1^2\sigma_2^2-|\rho|^2}\begin{bmatrix}\rho^H & \sigma_1^2\end{bmatrix}\begin{bmatrix}\sigma_2^2 & -\rho \\ -\rho^H & \sigma_1^2\end{bmatrix}\begin{bmatrix}\rho \\ \sigma_2^2\end{bmatrix} = \sigma_2^2. \end{aligned} \tag{8}$$

Combining (3), (4) and (8) we obtain:

$$\mathrm{CRB}(\delta) \approx \frac{\sigma^2}{2N\sigma_2^2}\cdot\frac{1}{\boldsymbol{d}_\delta^H\boldsymbol{\Pi}_{\boldsymbol{A}}^{\perp}\boldsymbol{d}_\delta} = \delta^2 \tag{9}$$

Finally, we obtain

$$\begin{aligned} \mathrm{SNR}_{\min} =&\frac{\sigma_2^2}{\sigma^2} = \frac{1}{2N\delta^2}\cdot\frac{1}{\boldsymbol{d}_\delta^H\boldsymbol{\Pi}_{\boldsymbol{A}}^{\perp}\boldsymbol{d}_\delta} \\ =&\frac{1}{2N\delta^2}\cdot\frac{M^2-|\boldsymbol{a}_\delta^H\boldsymbol{a}_1|^2}{Q}, \end{aligned} \tag{10}$$

where $Q = \mu k^2\cos^2(\theta_2)(M^2-|\boldsymbol{a}_\delta^H\boldsymbol{a}_1|^2) - M(|\boldsymbol{d}_\delta^H\boldsymbol{a}_1|^2 + |\boldsymbol{d}_\delta^H\boldsymbol{a}_\delta|^2) + 2\Re\{\boldsymbol{d}_\delta^H\boldsymbol{a}_\delta\boldsymbol{a}_\delta^H\boldsymbol{a}_1\boldsymbol{a}_1^H\boldsymbol{d}_\delta\}$, $\mu = \sum_{m=2}^{M} d_m^2$, $\boldsymbol{a}_1$ and $\boldsymbol{a}_\delta$ stand for $\boldsymbol{a}(\theta_1)$ and $\boldsymbol{a}(\theta_1+\delta)$, respectively. Note that, for the Uniform Linear Array (ULA) configuration, $\mu = \frac{M(M-1)(2M-1)}{6}d^2$, where d denotes the inter-sensor spacing.

4. SIMULATIONS AND NUMERICAL ANALYSIS

The context of our simulations is a ULA comprising $M = 6$ sensors with half-wave length inter-element spacing. The snapshot number is given by $N = 100$ and $\sigma_2^2 = 1$. The simulations reveal the following properties of the SRL in terms of $\mathrm{SNR}_{\min}$:

- In Fig. 1 we compare our approximate analytical expression of $\mathrm{SNR}_{\min}$ given by (10) with the exact numerical ones (given as the numerical solution of (4)) for signals with different values of the correlation. On the one hand, it demonstrates the validity of our approximation in (9) for a sufficient SNR, for which the analytical $\mathrm{SNR}_{\min}$ approaches the exact resolution limit. On the other hand, it is noticeable that according to our derived expression, the expression of $\mathrm{SNR}_{\min}$ is independent of ρ_c, i.e., the correlation between two signals. This means that ρ_c has no impact on the SRL for a sufficient SNR. This is also corroborated by Fig. 1, from which we see that only for low SNR cases ρ_c has a slight impact on $\mathrm{SNR}_{\min}$. We observe that signals with a higher ρ_c have a negligible better performance, whereas this impact gradually disappears as the SNR increases and is negligible for a high SNR.

- The results displayed in Fig. 2 demonstrate the behavior of $\mathrm{SNR}_{\min}$ w.r.t. different values of θ_1 and shows that the former is dependent on the latter. The statistical resolution limit in terms of $\mathrm{SNR}_{\min}$ increases as the value of θ_1 approaches $\frac{\pi}{2}$. Hence the broadside array directions have a improved resolution limit as compared to the end-fire directions, which matches our expectations.

- In Fig. 3 we compare $\mathrm{SNR}_{\min}$ given by (10) with $\mathrm{SNR}_{\min-\mathrm{root}}$ (i.e., the minimum SNR required to resolve two closely spaced source using the root-MUSIC scheme [3], which is obtained by applying the Smith criterion.) The figure demonstrates the validity of the former as a lower bound of the SNR required for the resolution.

- In Fig. 4 we investigate the impact of the sensor array geometry on $\mathrm{SNR}_{\min}$. Four types of array configurations are considered, as shown in Table 1. The result reveals that a loss of sensors in the array geometric configuration has a considerable impact on the $\mathrm{SNR}_{\min}$ only when it causes a diminution of the aperture size of the array, e.g., as in the case of the array Type 1 in Table 1. If, however, the array aperture remains unchanged, then the impact is considerably mitigated, e.g., as in the case of array Type 2 and Type 3. One can further notice that, by comparing the results given by Type 2 and Type 3, that a removal of sensors closer to the reference sensor causes a slightly higher $\mathrm{SNR}_{\min}$.

Array Type	Geometric Configuration
Type 1	○ ● ● ○ ● ● ○ ○
Type 2	● ● ○ ● ○ ○ ○ ●
Type 3	● ○ ○ ○ ○ ● ● ●
Type 4	● ● ● ● ● ● ● ●

Table 1. Different array geometric configurations. ● and ○ represent the position of sensor and missing sensors, respectively. The inter-element spacing is half-wave length.

5. CONCLUSIONS

In this paper we derived the statistical resolution in terms of a minimum SNR required to revolve two closely spaced signals. As a by-product, we also obtained the stochastic Cramér-Rao bound w.r.t. the separation between the DOA of the two signals. Both expressions are given in closed form and hence shed light on the behavior of $\mathrm{SNR}_{\min}$. Simulation results are provided to corroborate our analytical expressions and also to evaluate the properties of $\mathrm{SNR}_{\min}$ from various aspects. Our results confirm the intuition, that the $\mathrm{SNR}_{\min}$

[3] We use the root-MUSIC scheme as it is asymptotically efficient, and also for the purpose of simplicity.

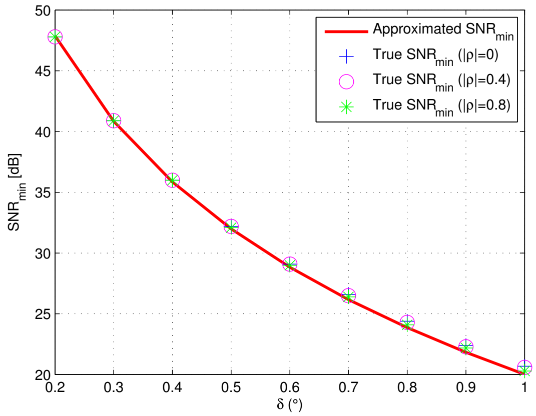

Fig. 1. $\mathrm{SNR}_{\min}$ (analytical) and $\mathrm{SNR}_{\min}$ (numerical with different ρ_c) vs. δ for $|\rho_c| = 0, 0.4, 0.8$.

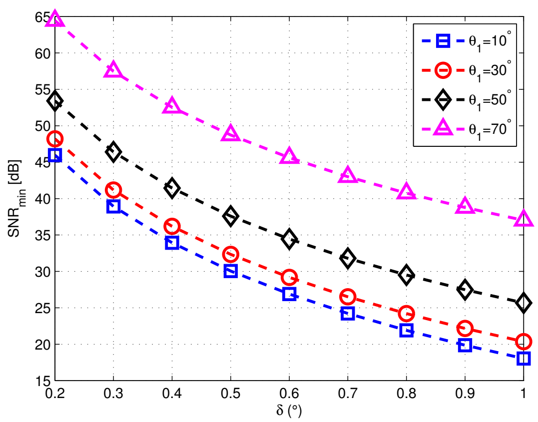

Fig. 2. $\mathrm{SNR}_{\min}$ vs. δ for $\theta_1 = 10°, 30°, 50°, 70°$.

depends on the direction of signals, in the sense that the resolution limit for signals at directions close to the broadside array is significantly better than for signals at the end-fire. We also noticed that the value of signal correlation has only negligible effect on the $\mathrm{SNR}_{\min}$. Finally, the impact of different array geometries on $\mathrm{SNR}_{\min}$ is investigated and discussed.

6. APPENDIX

In this appendix we demonstrate the outline of the derivation of CRB(δ), with the emphasis on the main steps and on all the steps that are different from [10] and [12].

Under the assumption **A1-A3**, the element in the i-th row of the k-th column of the FIM can be written as:

$$[\mathbf{FIM}(\boldsymbol{\xi})]_{i,k} = Ntr\left\{\frac{\partial \boldsymbol{R}}{\partial[\boldsymbol{\xi}]_i}\boldsymbol{R}^{-1}\frac{\partial \boldsymbol{R}}{\partial[\boldsymbol{\xi}]_k}\boldsymbol{R}^{-1}\right\}. \tag{11}$$

Using [10, eq. (7)-(9)] and after some mathematical manipulations, the whole FIM can be written and further parti-

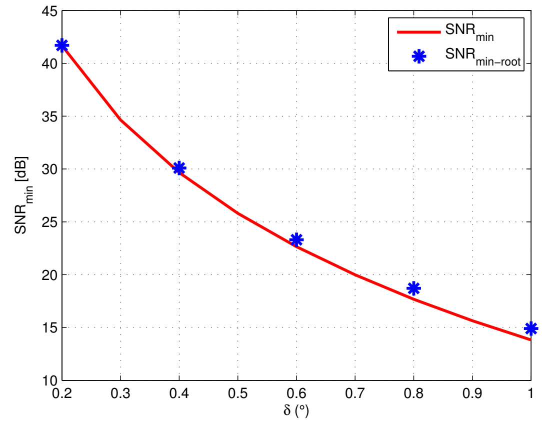

Fig. 3. $\mathrm{SNR}_{\min}$ and $\mathrm{SNR}_{\min-\mathrm{root}}$ vs. δ for $\theta_1 = 30°$. The trial number T=500.

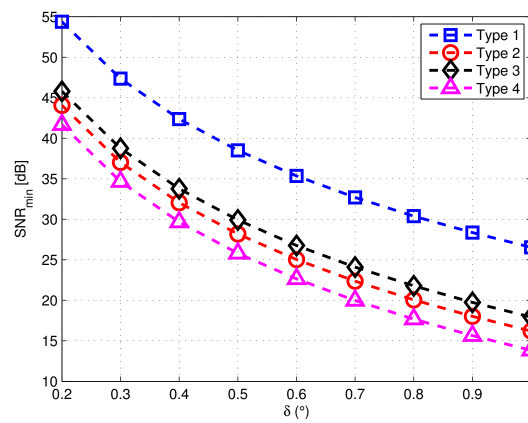

Fig. 4. $\mathrm{SNR}_{\min}$ vs. δ for different types of array configurations ($\theta_1 = 30°$).

tioned as follows:

$$\begin{aligned}\frac{1}{N}\mathbf{FIM}(\boldsymbol{\xi}) &= \left(\frac{\partial vec\{\boldsymbol{R}\}}{\partial \boldsymbol{\xi}^T}\right)^H (\boldsymbol{R}^{-T}\otimes\boldsymbol{R}^{-1})\left(\frac{\partial vec\{\boldsymbol{R}\}}{\partial \boldsymbol{\xi}^T}\right)\\ &\triangleq \left[\begin{array}{c|c}\boldsymbol{\gamma}^H\boldsymbol{\gamma} & \boldsymbol{\gamma}^H\boldsymbol{X}\\ \hline \boldsymbol{X}\boldsymbol{\gamma}^H & \boldsymbol{X}^H\boldsymbol{X}\end{array}\right],\end{aligned} \tag{12}$$

where $\boldsymbol{X} = [\boldsymbol{\Psi} \quad \boldsymbol{\upsilon}]$, $\boldsymbol{\gamma} = (\boldsymbol{R}^{-\frac{T}{2}}\otimes\boldsymbol{R}^{-\frac{1}{2}})\frac{\partial vec\{\boldsymbol{R}\}}{\partial\delta}$, $\boldsymbol{\Psi} = (\boldsymbol{R}^{-\frac{T}{2}}\otimes\boldsymbol{R}^{-\frac{1}{2}})\frac{\partial vec\{\boldsymbol{R}\}}{\partial\boldsymbol{\varsigma}^T}$, $\boldsymbol{\upsilon} = (\boldsymbol{R}^{-\frac{T}{2}}\otimes\boldsymbol{R}^{-\frac{1}{2}})\frac{\partial vec\{\boldsymbol{R}\}}{\partial\sigma^2}$.

Based on the above partition of the FIM and applying the Schur complement [13] on $\boldsymbol{\gamma}$, one obtains:

$$\begin{aligned}\mathrm{CRB}(\delta) &= \left[\mathbf{FIM}(\boldsymbol{\xi})^{-1}\right]_{1,1}\\ &= \frac{1}{N}\cdot\frac{1}{\boldsymbol{\gamma}^H\boldsymbol{\gamma}-\boldsymbol{\gamma}^H\boldsymbol{X}(\boldsymbol{X}^H\boldsymbol{X})^{-1}\boldsymbol{X}^H\boldsymbol{\gamma}}\\ &= \frac{1}{N}\cdot\frac{1}{\boldsymbol{\gamma}^H\boldsymbol{\Pi}_{\boldsymbol{X}}^{\perp}\boldsymbol{\gamma}},\end{aligned} \tag{13}$$

where $\mathbf{\Pi}_{\boldsymbol{X}}^{\perp}$ indicates the orthogonal projector onto the orthogonal complement of the subspace spanned by the columns of the matrix $\boldsymbol{X}$, i.e., $\mathbf{\Pi}_{\boldsymbol{X}}^{\perp} = \boldsymbol{I} - \boldsymbol{X}(\boldsymbol{X}^H\boldsymbol{X})^{-1}\boldsymbol{X}^H$.

Further, after some manipulations [10, eq. (16)], $\mathbf{\Pi}_{\boldsymbol{X}}^{\perp}$ can be expressed as

$$\mathbf{\Pi}_{\boldsymbol{X}}^{\perp} = \mathbf{\Pi}_{\mathbf{\Psi}}^{\perp} - \frac{\mathbf{\Pi}_{\mathbf{\Psi}}^{\perp}\boldsymbol{\upsilon}\boldsymbol{\upsilon}^H\mathbf{\Pi}_{\mathbf{\Psi}}^{\perp}}{\boldsymbol{\upsilon}^H\mathbf{\Pi}_{\mathbf{\Psi}}^{\perp}\boldsymbol{\upsilon}}, \tag{14}$$

where it can be proved that [12, eq. (28)]

$$\boldsymbol{\upsilon}^H\mathbf{\Pi}_{\mathbf{\Psi}}^{\perp}\boldsymbol{\gamma} = 0. \tag{15}$$

Combining (15) with (13) and (14), one obtains

$$\mathrm{CRB}(\delta) = \frac{1}{N} \cdot \frac{1}{\boldsymbol{\gamma}^H\mathbf{\Pi}_{\mathbf{\Psi}}^{\perp}\boldsymbol{\gamma}}. \tag{16}$$

On the other hand, the following equation holds [10, eq. (27)]:

$$\mathbf{\Pi}_{\mathbf{\Psi}}^{\perp}\boldsymbol{\gamma} = vec\left\{\mathbf{\Pi}_{\boldsymbol{R}^{-\frac{1}{2}}\boldsymbol{A}}^{\perp}\mathbf{\Xi}^H + \mathbf{\Xi}\mathbf{\Pi}_{\boldsymbol{R}^{-\frac{1}{2}}\boldsymbol{A}}^{\perp}\right\} \tag{17}$$

in which $\mathbf{\Xi} = \boldsymbol{R}^{-\frac{1}{2}}\boldsymbol{A}\boldsymbol{c}_\rho\boldsymbol{d}_\delta^H\boldsymbol{R}^{-\frac{1}{2}}$, with $\boldsymbol{c}_\rho$ denoting the second column of $\boldsymbol{S}$ and $\boldsymbol{d}_\delta = \frac{\partial \boldsymbol{a}(\theta_1+\delta)}{\partial\delta}$. Hence, one obtains

$$\begin{aligned}
\mathrm{CRB}(\delta) &= \frac{1}{N} \cdot \frac{1}{\boldsymbol{\gamma}^H\mathbf{\Pi}_{\mathbf{\Psi}}^{\perp}\boldsymbol{\gamma}} = \frac{1}{N} \cdot \frac{1}{\boldsymbol{\gamma}^H\mathbf{\Pi}_{\mathbf{\Psi}}^{\perp}\mathbf{\Pi}_{\mathbf{\Psi}}^{\perp}\boldsymbol{\gamma}} \\
=&\frac{1}{N} \cdot \frac{1}{2\Re\{tr\{\mathbf{\Pi}_{\boldsymbol{R}^{-\frac{1}{2}}\boldsymbol{A}}^{\perp}\mathbf{\Xi}^H\mathbf{\Pi}_{\boldsymbol{R}^{-\frac{1}{2}}\boldsymbol{A}}^{\perp}\mathbf{\Xi}^H\} + tr\{\mathbf{\Xi}\mathbf{\Pi}_{\boldsymbol{R}^{-\frac{1}{2}}\boldsymbol{A}}^{\perp}\mathbf{\Xi}^H\}\}} \\
=&\frac{1}{N} \cdot \frac{1}{2\Re\{tr\{\mathbf{\Xi}\mathbf{\Pi}_{\boldsymbol{R}^{-\frac{1}{2}}\boldsymbol{A}}^{\perp}\mathbf{\Xi}^H\}\}} \\
=&\frac{1}{N} \cdot \frac{1}{2\Re\{tr\{\boldsymbol{R}^{-\frac{1}{2}}\boldsymbol{A}\boldsymbol{c}_\rho\boldsymbol{d}_\delta^H\boldsymbol{R}^{-\frac{1}{2}}\mathbf{\Pi}_{\boldsymbol{R}^{-\frac{1}{2}}\boldsymbol{A}}^{\perp}\boldsymbol{R}^{-\frac{1}{2}}\boldsymbol{d}_\delta\boldsymbol{c}_\rho^H\boldsymbol{A}^H\boldsymbol{R}^{-\frac{1}{2}}\}\}} \\
=&\frac{1}{N} \cdot \frac{1}{2\Re\{(\boldsymbol{d}_\delta^H\boldsymbol{R}^{-\frac{1}{2}}\mathbf{\Pi}_{\boldsymbol{R}^{-\frac{1}{2}}\boldsymbol{A}}^{\perp}\boldsymbol{R}^{-\frac{1}{2}}\boldsymbol{d}_\delta)(\boldsymbol{c}_\rho^H\boldsymbol{A}^H\boldsymbol{R}^{-1}\boldsymbol{A}\boldsymbol{c}_\rho)\}}.
\end{aligned}$$

Note that $\boldsymbol{R}^{-\frac{1}{2}}\mathbf{\Pi}_{\boldsymbol{R}^{-\frac{1}{2}}\boldsymbol{A}}^{\perp}\boldsymbol{R}^{-\frac{1}{2}} = \frac{1}{\sigma^2}\mathbf{\Pi}_{\boldsymbol{A}}^{\perp}$ [12, eq. (31)], therefore

$$\begin{aligned}
\mathrm{CRB}(\delta) &= \frac{1}{N} \cdot \frac{\sigma^2}{2\Re((\boldsymbol{d}_\delta^H\mathbf{\Pi}_{\boldsymbol{A}}^{\perp}\boldsymbol{d}_\delta)(\boldsymbol{c}_\rho^H\boldsymbol{A}^H\boldsymbol{R}^{-1}\boldsymbol{A}\boldsymbol{c}_\rho))} \\
&= \frac{1}{N} \cdot \frac{\sigma^2}{2(\boldsymbol{d}_\delta^H\mathbf{\Pi}_{\boldsymbol{A}}^{\perp}\boldsymbol{d}_\delta)(\boldsymbol{c}_\rho^H\boldsymbol{A}^H\boldsymbol{R}^{-1}\boldsymbol{A}\boldsymbol{c}_\rho)} \\
&= \frac{\sigma^2}{2N} \cdot \frac{1}{\boldsymbol{d}_\delta^H\mathbf{\Pi}_{\boldsymbol{A}}^{\perp}\boldsymbol{d}_\delta\boldsymbol{c}_\rho^H\boldsymbol{A}^H\boldsymbol{R}^{-1}\boldsymbol{A}\boldsymbol{c}_\rho},
\end{aligned} \tag{18}$$

which concludes the proof.

References

[1] H. Krim and M. Viberg, "Two decades of array signal processing research: the parametric approach," *IEEE Signal Processing Mag.*, vol. 13, no. 4, pp. 67–94, 1996.

[2] S. T. Smith, "Statistical resolution limits and the complexified Cramér Rao bound," *IEEE Trans. Signal Processing*, vol. 53, pp. 1597–1609, May 2005.

[3] M. Shahram and P. Milanfar, "On the resolvability of sinusoids with nearby frequencies in the presence of noise," *IEEE Trans. Signal Processing*, vol. 53, no. 7, pp. 2579–2588, July 2005.

[4] M. N. El Korso, R. Boyer, A. Renaux, and S. Marcos, "Statistical resolution limit for multiple signals and parameters of interest," in *Proc. of IEEE Int. Conf. Acoust., Speech, Signal Processing*, Dallas, TX, 2010, vol. 3.

[5] H. Cox, "Resolving power and sensitivity to mismatch of optimum array processors," *J. Acoust. Soc.*, vol. 54, no. 3, pp. 771–785, 1973.

[6] M. Shahram and P. Milanfar, "On the resolvability of sinusoids with nearby frequencies in the presence of noise," *IEEE Trans. Signal Processing*, vol. 53, no. 7, pp. 2579–2585, July 2005.

[7] Z. Liu and A. Nehorai, "Statistical angular resolution limit for point sources," *IEEE Trans. Signal Processing*, vol. 55, no. 11, pp. 5521–5527, Nov. 2007.

[8] H. B. Lee, "The Cramér-Rao bound on frequency estimates of signals closely spaced in frequency," *IEEE Trans. Signal Processing*, vol. 40, no. 6, pp. 1507–1517, 1992.

[9] M. N. El Korso, R. Boyer, A. Renaux, and S. Marcos, "Statistical resolution limit of the uniform linear cocentered orthogonal loop and dipole array," *IEEE Trans. Signal Processing*, vol. 59, no. 1, pp. 425–431, Jan. 2011.

[10] M. Pesavento E. G. Larsson A. B. Gershman, P. Stoica, "Stochastic cramer-rao bound for direction estimation in unknown noise fields," *IEE Proceedings - Radar, Sonar and Navigation*, vol. 149.

[11] K.B. Petersen and M.S. Pedersen, "The matrix cookbook," *Citeseer*, 2006.

[12] A. B. Gershman P. Stoica, E. G. Larsson, "The stochastic CRB for array processing: a textbook derivation," *IEEE Signal Processing Letters*, vol. 8.

[13] G. H. Golub and C. F. Van Loan, *Matrix Computations*, Johns Hopkins, London, 1989.